Human Pathology (2019) **94**, 98–109

ELSEVIER

Human PATHOLOGY

www.elsevier.com/locate/humpath

Original contribution

Intratumoral heterogeneity and loss of ARID1A expression in gastric cancer correlates with increased PD-L1 expression in Western patients☆,☆☆

Julia Maria Tober MD, Christine Halske MD, Hans-Michael Behrens MSc, Sandra Krüger BSc, Christoph Röcken MD, PhD*

Department of Pathology, Christian-Albrechts-University, D-24105 Kiel, Germany

Received 24 August 2019; accepted 11 September 2019

Keywords:
Gastric carcinoma;
ARID1A;
PD-L1;
Immunohistochemistry;
Heterogeneity;
MSI

Summary Recent whole-genome sequencing showed frequent mutations of *ARID1A* in gastric cancer (GC). In this study of a large independent Central European cohort, we evaluated the expression of ARID1A in whole tissue sections (WTS) of GC testing the following hypotheses: ARID1A shows intratumoral heterogeneity, and ARID1A expression and/or heterogeneity correlates with clinicopathological patient characteristics. ARID1A expression was studied by immunohistochemistry in 450 primary GCs and 143 corresponding lymph node metastases. The expression pattern was correlated with clinicopathological characteristics and patient survival. *ARID1A* genotype and CpG methylation status were additionally analyzed in 7 GCs with a heterogeneous "black-and-white" expression pattern. ARID1A was expressed heterogeneously in 23 (5.1%) GCs, depicting a black-and-white pattern of negative and positive tumor areas. Complete loss of expression was found in 43 (9.6%) GCs. ARID1A status correlated significantly with tumor type according to Laurén, Epstein-Barr virus status, microsatellite instability, PD-L1 status, and nodal spread. There was no correlation with patient survival. In 4 cases with heterogeneous ARID1A expression, frame shift variants were detected. Summing up, heterogeneous or complete loss of ARID1A expression occurred in 14.7% of GCs and correlated with PD-L1 status, indicating potential for future combined anti–PD-L1/ARID1A therapy. In a subgroup of cases, ARID1A loss was heterogeneous, which suggests that *ARID1A* mutations might be a later event in gastric carcinogenesis.

1. Introduction

Worldwide, gastric cancer (GC) is the fifth most common malignancy and the third leading cause of cancer-related deaths. The prognosis is often poor because of initial diagnosis in advanced stages which necessitates chemotherapy and/or surgery. Histological classification of gastric adenocarcinoma, by far the

☆ Disclosures: The authors declare that they have no conflict of interest. This research did not receive any specific grant from funding agencies in the public, commercial, or not-for-profit sectors.

☆☆ Previous presentation: Data of this study were presented in part as a 10-minute oral presentation at the 101 Annual Meeting of the German Society of Pathology.

* Corresponding author at: Department of Pathology, Christian-Albrechts-University, Arnold-Heller-Str. 3, Haus U33, D-24105 Kiel, Germany.
E-mail address: christoph.roecken@uksh.de (C. Röcken).

https://doi.org/10.1016/j.humpath.2019.09.016

most common entity, according to either Laurén [1] or the World Health Organization [2] is of little practical use when it comes to multimodal oncological treatment. Thus, novel prognostic and/or predictive biomarkers are urgently needed to pave the way for new, more effective therapeutic concepts. This was further substantiated by the genetic complexity of GC, which was recently unraveled by integrative genomic analyses including whole-genome sequencing [3-5]. A molecular classification categorizing 4 subtypes (Epstein-Barr virus [EBV] positive, microsatellite instable [MSI], chromosomal instable, and genomically stable GC) was proposed [3].

ARID1A (synonymous: *BAF250a*) is a gene located on chromosome 1p36.11, which encodes for an identically named protein participating in the SWI/SNF (SWItch/Sucrose Non Fermentable) ATP-dependent genome remodeling complex [6]. The SWI/SNF complex regulates dynamic repositioning of nucleosomes, which makes mutational loss of any essential complex unit, such as ARID1A, highly likely to disrupt potentially a very large number of nuclear processes (eg, transcription, DNA replication, and DNA damage repair) via several different signaling pathways [7]. ARID1A has been established as a tumor suppressor gene [8,9] with frequent mutations in various human cancers, for example, ovarian clear cell carcinoma, endometrial carcinomas [6,10], and also GC [11]. With regard to patient survival, data are still contradictory. In previous studies, altered ARID1A expression was found to correlate with improved patient outcome [12] or worse outcome [13] or did not correlate with patient survival at all [4]. The exact mechanisms with which ARID1A effects downstream signaling cascades and processes have not been fully explored; however, some pathways have been found: for instance, Trizzino et al have shown that, in ovarian clear cell carcinoma, ARID1A loss impairs pausing of RNA polymerase II (RNAP II), resulting in transcriptional dysregulation of active genes. The authors showed that, whereas some of the effects were counteracted by increased ARID1B expression, some genes, such as *TP53*, were exclusively dependent on ARID1A [14]. The close connection of ARID1A and *TP53* has also been shown by Guan et al for ovarian cancers [15]. Like p53, ARID1A's downstream effects are achieved by regulating CDKN1A and SMAD3 with ARID1A forming a complex with BRG1, with its effects being mediated by p53 [15]. Ashizawa et al [13] showed an inverse correlation of ARID1A expression with PD-L1 and p53 expression in an Asian patient cohort, which—to the best of the authors' knowledge—has not yet been confirmed for a European patient cohort outside of this study.

Along with aiming to validate ARID1A independently for GC in a large, extensively characterized central European cohort, we sought to test the following hypotheses: (1) ARID1A shows intratumoral heterogeneity, and (2) ARID1A expression correlates with clinicopathological patient characteristics, including EBV, MSI, and PD-L1 status and patient outcome.

2. Materials and methods

2.1. Study population

From the archive of the Institute of Pathology, University Hospital Kiel, we sought patients who had undergone either total or partial gastrectomy for adenocarcinoma of the stomach or esophagogastric junction between 1997 and 2009. Informed consent or similar was obtained from each patient. The following patient characteristics were retrieved: type of surgery, age at diagnosis, sex, tumor size, tumor localization, tumor type, tumor grade, depth of invasion, residual tumor status, number of lymph nodes resected, and number of lymph nodes with metastases. Patients were included if an adenocarcinoma of the stomach or esophagogastric junction was histologically confirmed. Exclusion criteria were defined as (1) histology identified a tumor type other than adenocarcinoma, (2) patients had undergone perioperative chemo- or radiotherapy and (3) the tumor had developed in the residual stomach after Billroth resection. Each resected specimen had undergone gross sectioning and histological examination by trained and board-certified surgical pathologists. Date of patient death was obtained from the *Epidemiological Cancer Registry* of the state of Schleswig-Holstein, Germany. Follow-up data of those patients who were still alive were retrieved from hospital records and general practitioners. Ethical approval was obtained from the local ethical review board (D 453/10). All patient data were pseudonymized prior to study inclusion.

2.2. Histology

Tissue specimens were fixed in formalin and embedded in paraffin (FFPE). Deparaffinized sections were stained with hematoxylin and eosin. Histological reexamination of primary tissue sections was carried out for all cases to ensure that inclusion criteria were confirmed. Tumors had previously been classified according to the Laurén classification and reexamined by 2 surgical pathologists. pTNM stage of all study patients was determined according to the eighth edition of the Union for International Cancer Control (UICC) guidelines.

2.3. Assessment of microsatellite instability and detection of *Helicobacter pylori* and Epstein-Barr virus infection

The *H pylori*, microsatellite instability, Epstein-Barr virus, HER2, MET, *PIK3CA*, PD-L1, and PD-1 status was assessed as described in previous studies [16-20].

2.4. Immunohistochemical detection of *ARID1A*

Immunohistochemical stainings were carried out on tissue sections of the primary tumor and lymph node metastases

using the Bondmax (Leica Biosystems, Wetzlar, Germany), an automated slide staining system. Pretreatment was done with ER2 (Leica Biosystems) for 30 minutes. A monoclonal rabbit antibody, directed against ARID1A/ BAF250A (clone D2A8U; Cell Signaling Technology, Cambridge, United Kingdom) was applied in a 1:100 dilution. For visualization, the Polymer Refine Detection Kit (Menarini Diagnostics, Berlin, Germany) was used.

2.5. Evaluation of ARID1A immunostaining

Nuclear expression of ARID1A was evaluated using the histoscore (H-score): The first parameter was based on the intensity of the stained cells. A score of 0 (no staining), 1+ (weak), 2+ (moderate), and 3+ (strong staining reaction) was applied (Fig. 1).

The second parameter estimated the distribution of the stained cells in percentage. The sum total of all staining intensities found in a single case always added to a total of 100% according to the following formula: % (0) + % (1+) + % (2+) + % (3+) = 100%. Finally, the H-score was calculated according to the following formula: 0 × (% of immunonegative tumor cells) + 1 × (% of weakly stained tumor cells) + 2 × (% of moderately stained tumor cells) + 3 × (% of strongly stained tumor cells) = H-score. The H-score ranged from 0 [= 0 × (100% immunonegative tumor cells)] to 300 [= 3 × (100% of strongly stained tumor cells)].

Additionally, cases of GC depicting a heterogeneous "black-and-white" (b/w) expression pattern were identified and marked separately. The *b/w pattern* was defined as to 2 or more clearly separated areas of completely negative and positive tumor (of any staining intensity) within the same

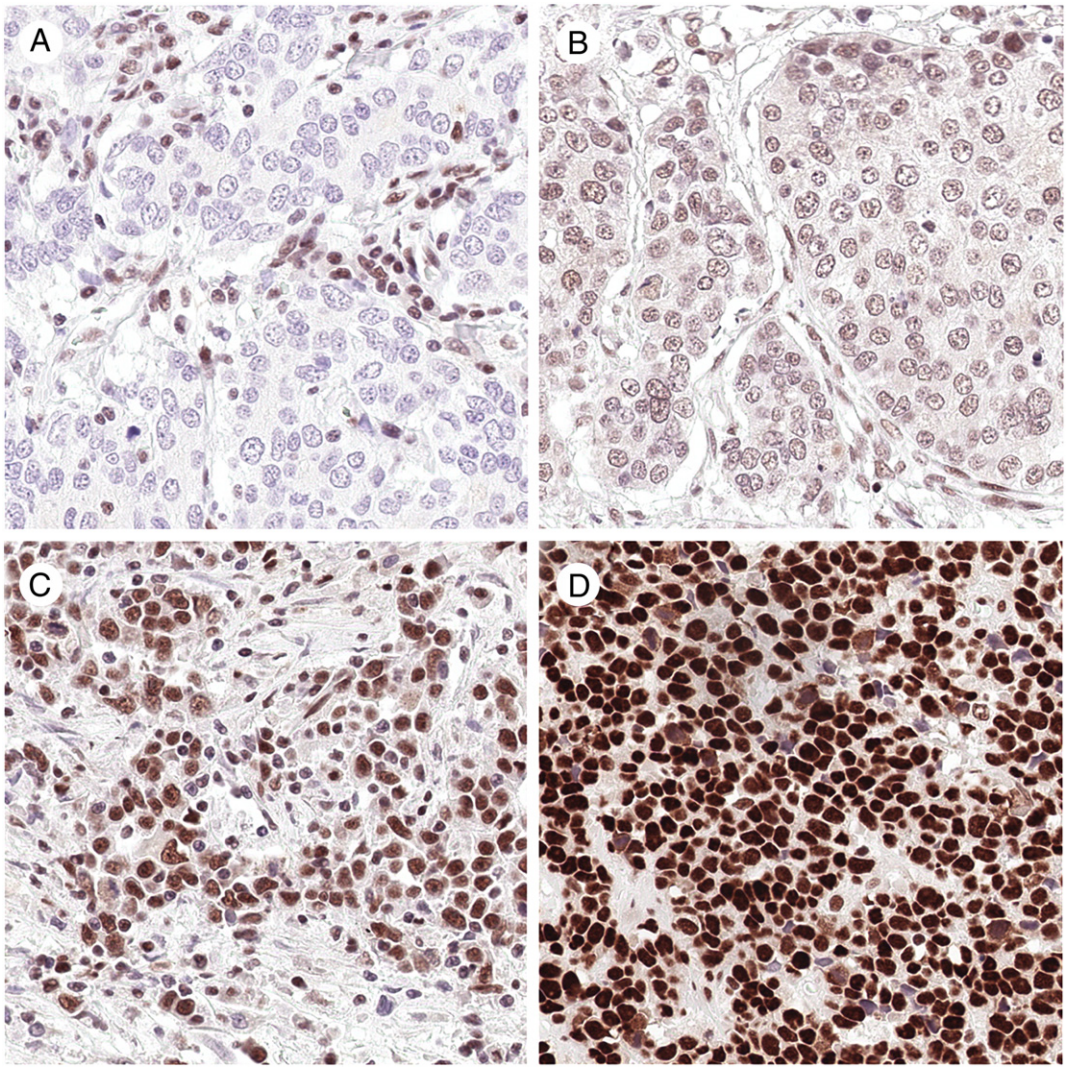

Fig. 1 References for immunostaining analysis according to H-score. Staining intensities ranged from 0 (A; negative) to 3+ (D, strong expression) with 1+ (B; weak expression) and 2+ (C; moderate expression) in between. Lymphocytes served as internal positive control. Anti-ARID1A immunostaining, hematoxylin counterstain; original magnification ×400.

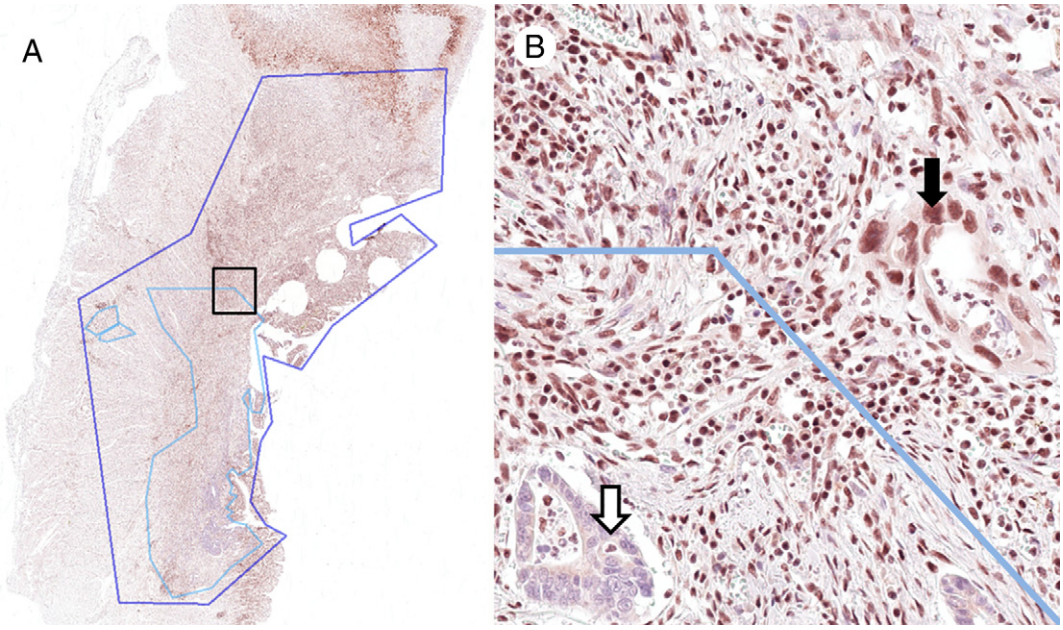

Fig. 2 For the analysis of the percentage of positive and negative ARID1A expression in gastric cancer with a b/w expression pattern, immunostained gastric cancer slides were scanned and digitally analyzed. A, Prior to analysis, complete tumor area (dark blue) and negative tumor areas (light blue) were manually marked (×8.75). B, excert at ×200 magnification (⬇ positive tumor, ⇩ negative tumor in tubular formations). Anti-ARID1A immunostaining, hematoxylin counterstain.

tumor (Fig. 2, Supplementary Fig. 3). Single negative tumor cells diffusely intermixed with positive tumor cells were not classified as heterogeneous b/w cases.

2.6. Digital evaluation of percentage of negative tumor area

All GCs depicting a heterogeneous b/w expression pattern were scanned using the Leica SCN 400 slide scanner. In a second step, the entire tumor area and the negative area(s) were digitally marked. The percentage of negative tumor area in each case was calculated using a specifically developed viewer program with annotation drawing capabilities and area calculation routines (VMP; Fig. 2).

2.7. Mutation and hypermethylation analysis

Out of 23 GCs depicting a heterogeneous b/w expression pattern, 7 were suitable with regard to the quality and amount of DNA extracted from FFPE tissue specimens to be tested for *ARID1A* gene mutations. For each case, areas with positive and negative ARID1A immunostaining were marked separately. The corresponding areas were manually microdissected from FFPE tissue sections, and DNA was extracted using the DNA mini kit (Qiagen, Hilden, Germany). For DNA quality check, a qualitative size range polymerase chain reaction (PCR) assay was done. Only cases with fragments larger than 300 base pairs were used for next-generation sequencing (NGS) analysis. The DNA quality of 16 cases was insufficient for NGS. DNA concentrations were measured using the Qubit dsDNA BR assay kit on a Qubit fluorometer 3.0 (Life Technologies, Carlsbad, CA). For exon analysis of *ARID1A*, an NGS amplicon custom assay was designed with DesignStudio (Illumina, SanDiego, U.S.A.) consisting of 73 amplicons with an average size of 175 base pairs. Target enrichment was performed using the TruSeq Custom Amplicon low Input dual pool (Illumina) workflow following the manufactures instruction. The pooled libraries were paired-end (2×151) sequenced on a micro flow cell with V2 chemistry on a MiSeq instrument (Illumina). Data analysis was performed using the MiSeqReporter Software and VariantStudio (both Illumina). A minimal amplicon coverage of 500 and a variant allele frequency of 5% were defined. Single nucleotide variants (SNVs) were subsequently validated with Sanger sequencing (by dye terminator cycle sequencing). Primer sequences used for amplification are shown in Supplementary Table 1. PCR products were purified using the Nucleospin Extract II kit (Macherey-Nagel, Düren, Germany) and sequenced with PCR primer and the BigDye Terminator v1.1 Cycle Sequencing kit (Life Technologies, Darmstadt, Germany). The sequencing products were purified using the NucleoSEQ kit (Macherey-Nagel) and analyzed on a 3500 Genetic Analyzer (Life Technologies).

In a second step, hypermethylation analysis of the *ARID1A* CpG islands was done using the PyroMark CpG Assays HS_ARID1A_01_PM, HS_ARID1A_02_PM and HS_ARID1A_03_PM in combination with the PyroPCR Kit (all Qiagen). For DNA extraction and bisulfite conversion, the EpiTect Fast Bisulfite Kit (Qiagen) was used following the manufacturer's instructions. Pyrosequencing analysis of CpG

methylation was done using the PyroMark Q24 System and the PyroMark analysis software (Qiagen).

2.8. Statistical analysis

Statistical analyses were done using SPSS 24.0 (IBM Corporation, Armonk, NY). First, the H-score was dichotomized at the median (≤135 H-score versus >135 H-score; Supplementary Table 2), separating the data into a group with weak/negative and moderate/strong expression of ARID1A. To test our hypotheses, we then performed subgroup analyses of complete loss of ARID1A expression (H-score = 0) versus any staining (H-score> 0), heterogeneous b/w expression pattern, and a combined group of these 2 groups (complete or partial, heterogeneous loss of ARID1A expression). The significance of correlation between the subgroups and clinicopathological characteristics was calculated using Fisher exact test. To compensate false discovery rate within the correlations, we applied the Simes (Benjamini-Hochberg) procedure (multiple testing correction). Median overall survival and tumor-specific survival were determined using the Kaplan-Meier method, and log-rank test was used to determine significance of difference. For parameters of ordinal scale (T-category, N-category, UICC stage), we applied Kendall tau test additionally. To determine the influence of ARID1A on survival independently of other clinicopathological patient characteristics, we performed Cox regression analysis. Variables which tested significantly in univariate Cox regression analysis ($P < .05$) were included in the multivariate Cox regression analysis.

3. Results

In total, 450 patients fulfilled all study criteria. The clinicopathological patient characteristics are summarized in Table 1. According to Laurén, an intestinal phenotype was found in 228 (50.7%), a diffuse type in 141 (31.3%), a mixed type in 30 (6.7%), and an unclassifiable type in 50 (11.1%) patients. Overall survival data were available in 438 of 450 cases (97.3%) and tumor-specific survival data in 410 of 450 cases (91.1%). Mean follow-up period was 13.2 months (range 0-142.7 months; Table 1).

For 435 GCs, both EBV and MSI status was available with 35 (7.8%) MSI GCs and 19 (4.2%) EBV-positive GCs. MSI and EBV were mutually exclusive. One hundred nine (24.2%) GCs were classified as PD-L1 positive in tumor cells, and 159 (35.3%) GCs were classified as PD-L1 positive in tumor-infiltrating immune cells. PD-1 was expressed in tumor-infiltrating immune cells of 242 GCs (53.8%; Table 1).

3.1. ARID1A immunostaining

Nuclear expression of ARID1A was observed in tumor cells, stromal cells, endothelium, and non-neoplastic as well as in metaplastic epithelium and most prominently and consistently in lymphocytes which served as an internal positive control. The percentage of stained tumor cells ranged from 0% to 100% (median 95.0%). Staining intensities ranged from 0 to 3 with intensities 0, 1, 2, and 3 found in 80.4%, 90.2%, 85.6%, and 50.7% of all cases, respectively (Fig. 1). The H-score ranged from 0 to 275 with a median of 136 (Supplementary Fig. 1).

3.1.1. ARID1A expression patterns

In WTS of primary GCs, 3 distinct expression patterns of ARID1A were observed. A vast majority of 384 (85.4%) cases showed a diffusely distributed expression pattern of different ARID1A staining intensities within the same tumor (Supplementary Fig. 2A), 43 (9.5%) of 450 specimens depicted a homogeneous complete loss of ARID1A expression, and 23 (5.1%) cases showed a heterogeneous expression pattern of ARID1A with clearly demarcated positive and negative tumor areas (b/w pattern; Supplementary Fig. 2B and C).

3.1.2. Gastric cancer with heterogeneous ARID1A expression

Subsequently, we determined whether the size of the tumor area with a complete loss of ARID1A expression correlates with clinicopathological patient characteristics. We digitally calculated the percentage of positive and negative tumor areas in all 23 cases with a heterogeneous b/w expression pattern of ARID1A (Fig. 2). The median value of the ARID1A negative tumor area was 31.2% (range 1.0%-88.0%; standard deviation 28.2). There was no significant correlation between any clinicopathological patient characteristic and the percentage area of ARID1A loss in GC (data not shown).

3.1.3. ARID1A expression in corresponding lymph node metastases

Next, we compared the expression of ARID1A in primary tumors with its expression in the corresponding lymph node metastases. For this purpose, 143 lymph node metastases obtained from 24 GCs with at least partial loss of ARID1A in the primary tumor were analyzed. Seventeen (70.8%) primary GCs (case #1-17) showed a complete loss of ARID1A, and 7 (29.2%) primary GCs (case #18-24) showed a heterogeneous b/w expression pattern (Supplementary Fig. 3). Overall, 115 (80.4%) lymph node metastases depicted a complete loss of ARID1A. These included 96 lymph node metastases obtained from 17 patients with complete loss of ARID1A in the primary tumor (case #1-17). Of the 47 lymph node metastases of 7 patients with heterogeneous ARID1A expression in the primary tumor, 24 (51.1%) showed a complete loss of ARID1A, 10 (21.3%) retained expression, and 13 (27.6%) showed a heterogeneous expression in the lymph node metastases. The 10 positive nodal metastases belonged to the same primary tumor, so did the 12 heterogeneous metastases. Among the latter, 3 nodal metastases showed heterogeneity in a b/w pattern and 9 in a diffuse way. Nodal metastases of the same primary GC always depicted the same expression pattern or loss.

Table 1 Clinicopathological patient characteristics and correlation with ARID1A expression

	Total		Complete ARID1A loss vs ARID1A expression				ARID1A b/w vs non-b/w				ARID1A H-score = 0 or b/w vs rest			
	Valid		H-score = 0		H-score > 0		B/w pattern		No b/w pattern		H-score = 0 or b/w		H-score > 0 and no b/w	
			Valid		P		Valid		P		Valid		P	
	n	(%)	n	(%)	n	(%)	n	(%)	n	(%)	n	(%)	n	(%)
Sex	450	(100)	427			.743 [a]	407			.380 [a]	450			.786 [a]
Female	171	(38.0)	15	(9.4)	145	(90.6)	11	(7.1)	145	(92.9)	26	(15.2)	145	(84.8)
Male	279	(62.0)	28	(10.5)	239	(89.5)	12	(4.8)	239	(95.2)	40	(14.3)	239	(85.7)
Age group	450	(100)	407			.529 [a]	407			.529 [a]	450			1.000 [a]
<68 y	227	(50.4)	23	(10.6)	194	(89.4)	10	(4.9)	194	(95.1)	33	(14.5)	194	(85.5)
≥68 y	223	(49.6)	20	(9.5)	190	(90.5)	13	(6.4)	190	(93.6)	33	(14.8)	190	(85.2)
Localization	450	(100)	427			.016 [a,d]	407			.486 [a]	450			.152 [a]
Proximal	142	(31.6)	21	(15.3)	116	(84.7)	5	(4.1)	116	(95.9)	26	(18.3)	116	(81.7)
Distal	308	(68.4)	22	(7.6)	268	(92.4)	18	(6.3)	268	(93.7)	40	(13.0)	268	(87.0)
Laurén phenotype	449	(99.8)	426			.000 [a]	406			.037 [a,d]	449			.000 [a]
Intestinal	228	(50.7)	23	(10.7)	191	(89.3)	14	(6.8)	191	(93.2)	37	(16.2)	191	(83.8)
Diffuse	141	(31.3)	6	(4.3)	132	(95.7)	3	(2.2)	132	(97.8)	9	(6.4)	132	(93.6)
Mixed	30	(6.7)	1	(3.4)	28	(96.6)	1	(3.4)	28	(96.6)	2	(6.7)	28	(93.3)
Unclassified	50	(11.1)	13	(28.9)	32	(71.1)	5	(13.5)	32	(86.5)	18	(36.0)	32	(64.0)
Grade	449	(99.8)	426			.132 [a]	406			1.000 [a]	449			.276 [a]
G1/G2	109	(24.2)	6	(5.8)	97	(94.2)	6	(5.8)	97	(94.2)	12	(11.0)	97	(89.0)
G3/G4	340	(75.6)	37	(11.5)	286	(88.5)	17	(5.6)	286	(94.4)	54	(15.9)	286	(84.1)
T category	450	(100)	427			.869 [a]	407			.699 [a]	450			.953 [a]
T1	53	(11.8)	4	(8.0)	46	(92.0)	3	(6.1)	46	(93.9)	7	(13.2)	46	(86.8)
T2	54	(12.0)	5	(10.0)	45	(90.0)	4	(8.2)	45	(91.8)	9	(16.7)	45	(83.3)
T3	184	(40.9)	16	(9.2)	158	(90.8)	10	(6.0)	158	(94.0)	26	(14.1)	158	(85.9)
T4	159	(35.3)	18	(11.8)	135	(88.2)	6	(4.3)	135	(95.7)	24	(15.1)	135	(84.9)
N category	449	(99.8)	426			.012 [a]	406			.014 [a]	449			.003 [a]
N0	131	(29.1)	14	(11.7)	106	(88.3)	11	(9.4)	106	(90.6)	25	(19.1)	106	(80.9)
N1	63	(14.0)	8	(14.0)	49	(86.0)	6	(10.9)	49	(89.1)	14	(22.2)	49	(77.8)
N2	81	(18.0)	13	(16.3)	67	(83.8)	1	(1.5)	67	(98.5)	14	(17.3)	67	(82.7)
N3(a/b)	174	(38.7)	8	(4.7)	161	(95.3)	5	(3.0)	161	(97.0)	13	(7.5)	161	(92.5)
M category	450	(100)	427			.837 [a]	407			.103 [a]	450			.506 [a]
M0	361	(80.2)	36	(10.4)	310	(89.6)	15	(4.6)	310	(95.4)	51	(14.1)	310	(85.9)
M1	89	(19.8)	7	(8.6)	74	(91.4)	8	(9.8)	74	(90.2)	15	(16.9)	74	(83.1)
UICC stage	450	(100)	427			.851 [a]	407			.000 [a]	450			.145 [a]
IA/B	77	(17.1)	6	(8.3)	66	(91.7)	5	(7.0)	66	(93.0)	11	(14.3)	66	(85.7)
IIA/B	99	(22.0)	11	(12.2)	79	(87.8)	9	(10.2)	79	(89.8)	20	(20.2)	79	(79.8)
IIIA/B/C	187	(41.6)	19	(10.2)	167	(89.8)	1	(0.6)	167	(99.4)	20	(10.7)	167	(89.3)
IV	87	(19.3)	7	(8.9)	72	(91.1)	8	(10.0)	72	(90.0)	15	(17.2)	72	(82.8)
L category	434	(96.4)	413			.032 [a,d]	394			.379 [a]	434			.028 [a,d]
L0	213	(47.3)	26	(12.9)	175	(87.1)	12	(6.4)	175	(93.6)	38	(17.8)	175	(82.2)
L1	221	(49.1)	14	(6.6)	198	(93.4)	9	(4.3)	198	(95.7)	23	(10.4)	198	(89.6)
LNR	448	(99.6)	425			.002 [a]	405			.090 [a]	448			.001 [a]
<Median	224	(49.8)	31	(14.8)	178	(85.2)	204	(96.2)	8	(3.8)	204	(91.1)	20	(8.9)
≥Median	224	(49.8)	12	(5.6)	204	(94.4)	178	(92.2)	15	(7.8)	178	(79.5)	46	(20.5)
V category	434	(96.4)	413			.605 [a]	394			.491 [a]	434			.278 [a]
V0	384	(85.3)	37	(10.2)	327	(89.8)	20	(5.8)	327	(94.2)	57	(14.8)	327	(85.2)
V1	50	(11.1)	3	(6.1)	46	(93.9)	1	(2.1)	46	(97.9)	4	(8.0)	46	(92.0)
R status	448	(99.6)	425			.825 [a]	405			.754 [a]	448			.541 [a]
R0	394	(87.6)	39	(10.5)	334	(89.5)	21	(5.9)	334	(94.1)	60	(15.2)	334	(84.8)
R1/R2	54	(12.0)	4	(7.7)	48	(92.3)	2	(4.0)	48	(96.0)	6	(11.1)	48	(88.9)
Helicobacter pylori status	364	(85.3)	367			.238 [a]	346			1.000 [a]	384			.166 [a]
Negative	324	(72.0)	35	(11.3)	274	(88.7)	15	(5.2)	274	(94.8)	50	(15.4)	274	(84.6)
Positive	60	(13.3)	3	(5.2)	55	(94.8)	2	(3.5)	55	(96.5)	5	(8.3)	55	(91.7)
EBV status	435	(96.7)	412			.011 [a]	394			.006 [a]	435			.001 [a]

Table 1 (*continued*)

	Total		Complete ARID1A loss vs ARID1A expression				ARID1A b/w vs non-b/w				ARID1A H-score = 0 or b/w vs rest			
	Valid		H-score = 0		H-score > 0		B/w pattern		No b/w pattern		H-score = 0 or b/w		H-score > 0 and no b/w	
			Valid		P		Valid		P		Valid		P	
	n	(%)	n	(%)	n	(%)	n	(%)	n	(%)	n	(%)	n	(%)
Negative	416	(92.4)	36	(9.1)	361	(90.9)	19	(5.0)	361	(95.0)	55	(13.2)	361	(86.8)
Positive	19	(4.2)	5	(33.3)	10	(66.7)	4	(28.6)	10	(71.4)	9	(47.4)	10	(52.6)
MSI status	435	(96.7)	412			.000 [a]	394			.004 [a]	435			.000 [a]
MSS	400	(88.9)	26	(6.8)	356	(93.2)	18	(4.8)	356	(95.2)	44	(11.0)	356	(89.0)
MSI	35	(7.8)	15	(50.0)	15	(50.0)	5	(25.0)	15	(75.0)	20	(57.1)	15	(42.9)
HER2 status	423	(94.0)	401			1.000 [a]	383			.708 [a]	423			.631 [a]
Negative	387	(86.0)	37	(10.1)	329	(89.9)	21	(6.0)	329	(94.0)	58	(15.0)	329	(85.0)
Positive	36	(8.0)	3	(8.6)	32	(91.4)	1	(3.0)	32	(97.0)	4	(11.1)	32	(88.9)
MET status	439	(97.6)	416			.341 [a]	396			1.000 [a]	439			.287 [a]
Negative	409	(90.9)	42	(10.9)	345	(89.1)	22	(6.0)	345	(94.0)	64	(15.6)	345	(84.4)
Positive	30	(6.7)	1	(3.4)	28	(96.6)	1	(3.4)	28	(96.6)	2	(6.7)	28	(93.3)
PIK3CA genotype	441	(98.0)	418			.402 [a]	398			.000 [a]	441			.001 [a]
Wild type	417	(92.7)	40	(10.0)	361	(90.0)	16	(4.2)	361	(95.8)	56	(13.4)	361	(86.6)
Mutated	24	(5.3)	3	(17.6)	14	(82.4)	7	(33.3)	14	(66.7)	10	(41.7)	14	(58.3)
PD-L1 in tumor cells	442	(98.2)	419			.000 [a]	400			.036 [a,d]	442			.000 [a]
Negative	333	(74.0)	17	(5.3)	302	(94.7)	75	(75.0)	25	(25.0)	31	(9.3)	302	(90.7)
Positive	109	(24.2)	25	(25.0)	75	(75.0)	9	(10.7)	75	(89.3)	34	(31.2)	75	(68.8)
PD-L1 in immune cells	442	(98.2)	419			.237 [a]	400			.822 [a]	442			.486 [a]
Negative	283	(62.9)	23	(8.6)	244	(91.4)	16	(6.2)	244	(93.8)	39	(13.8)	244	(86.2)
Positive	159	(35.3)	19	(12.5)	133	(87.5)	7	(5.0)	133	(95.0)	26	(16.4)	133	(83.6)
PD-1 in immune cells	445	(98.9)	442			.014 [a]	403			.016 [a,d]	445			.001 [a]
Negative	203	(45.1)	12	(6.1)	186	(93.9)	5	(2.6)	186	(97.4)	17	(8.4)	186	(91.6)
Positive	242	(53.8)	30	(13.4)	194	(86.6)	18	(8.5)	194	(91.5)	48	(19.8)	194	(80.2)
TSS (mo)	410	91.1	410			.105 [b] [c]	410			.275 [b]	410			.443 [b]
Total/events/censored	410/281/129		41/23/18		369/258/111		22/17/5		388/264/124		63/40/23		347/241/106	
Median survival	17.2 ± 1.5		29.8 ± 11.6		16.7 ± 1.6		17.9 ± 9.6		17.1 ± 1.6		21.5 ± 6.3		16.6 ± 1.6	
95% CI	[14.2-20.2]		[7.1-52.4]		[13.6-19.8]		[0.0-36.8]		[13.9-20.2]		[9.0-33.9]		[13.4-19.8]	

Abbreviation: TSS tumor-specific survival.

[a] Fisher exact test.

[b] Log-rank test.

[c] Kendall tau.

[d] Insignificant after multiple testing correction.

In conclusion, the lymph node metastases of 22 (93.7%) GCs showed complete loss of ARID1A expression, 1 (4.2%) GC had metastases with retained expression, and the metastases of 1 (4.2%) GC depicted heterogeneous expression, partly in a b/w pattern and partly diffusely (Supplementary Fig. 3).

3.2. Mutation analysis

Next, we tested whether heterogeneous ARID1A expression is related to genetic or epigenetic changes in terms of mutations and CpG hypermethylation. In 7 cases with heterogeneous ARID1A epression, DNA of sufficient quantity and quality was available for molecular testing. In 4 heterogeneous (b/w) cases (n = 4, 57%), we found frame shift variants (c.1644_1645insC, c.4550delC, c.3276_3277insA, and c.2179_2189delCGGCCACCCAG) in both areas (positive and negative) of the extracted regions. All SNVs are located in homopolymeric regions of the *ARID1A* gene. Three cases (n = 3, 43%) had no mutation in either area of ARID1A expression (wild type). We found no intratumoral heterogeneity and no methylation within *ARID1A* CpG islands.

3.3. Correlation with clinicopathological patient characteristics

To explore the putative biological significance of ARID1A in GC, we correlated its expression pattern with various clinicopathological patient characteristics (Table 1). However, in view of a heterogeneous expression and because we did not know a priori which "cutoff" value

of ARID1A expression might be biologically relevant, we applied a stepwise explorative approach:

First, we correlated the ARID1A expression according to the H-score dichotomized at the median (H-score ≤ 135 versus H-score> 135) with the clinicopathological patient characteristics. With the exception of the M category (P = .033), the resection status (P = .043), and the EBV status (P = .034), no correlation was found with any other parameter (Supplementary Table 2).

In a second step, we dichotomized the cohort into any staining (ie, weak, moderate or strong; H-score > 0) and complete loss of ARID1A (H-score = 0). Following this categorization, ARID1A loss correlated significantly with the phenotype according to Laurén, nodal spread, and lymph node ratio (Table 1). Complete loss of ARID1A expression was also significantly more commonly found in EBV-positive and in MSI GCs, respectively. Concordantly, ARID1A-negative GCs were also significantly more commonly PD-L1 and PD-1 positive, respectively (Table 1).

In a third step, we compared the GCs with b/w expression of *ARID1A* and without b/w expression. Cases with complete loss of ARID1A expression were excluded from this analysis (Table 1). Interestingly, partial loss of ARID1A expression (b/w) also correlated with the phenotype according to Laurén (P = .037; insignificant after correction for multiple testing), nodal spread (P = .014), tumor stage according to UICC (P .001), EBV, and MSI status (P = .006 and P = .004). Again, GCs with partial loss of ARID1A also significantly more commonly expressed PD-L1 (P = .036) and PD-1 (P = .016), respectively. Interestingly, no correlation was found with tumor localization.

Finally, we combined GCs with complete (H-score = 0) and partial (b/w) loss of ARID1A. Again, partial (b/w) or complete loss of ARID1A correlated with phenotype according to Laurén (P < .001), nodal spread (P = .003), lymph node ratio (P = .001), EBV (P = .001), and MSI status (P < .001; Table 1). Complete or partial loss of ARID1A expression also significantly correlated with *PIK3CA* genotype (P = .001), PD-L1- (P < .001), and PD-1 status (P = .001; Table 1).

3.4. Univariate survival analysis

Tumor-specific and overall survival of patients depended significantly on several clinicopathological parameters as well as some biomarkers (Laurén phenotype; T, M, N, V, and L category; lymph node ratio; UICC stage; tumor grade; R status; MSI status; PD-L1). ARID1A expression according to H-score, and complete or partial loss showed no correlation with patient survival (Table 2; Fig. 3).

3.5. Multivariate survival analysis (Cox regression)

A Cox regression analysis was performed on all parameters scoring a P < .05 in univariate analysis, that is, Laurén phenotype; L, V, G, and R category; UICC stage; lymph node ratio; tumor grade; and MSI status. Four parameters remained in the Cox model after running the backward LR method with P_{in} = .05 and P_{out} = .05. These were UICC stage, lymph node ratio, R status, MSI status, and PD-L1 status in immune cells. For tumor-specific survival, MSI status remained as a fifth parameter in the Cox model (Table 2, Supplementary Table 3).

4. Discussion

Comprehensive molecular characterization of solid organ tumors holds promise to open new avenues for future diagnostics and precision medicine. However, these findings necessitate validation studies of independent patient cohorts to provide solid grounds for future applications in a clinical context.

Recently, *ARID1A* was shown to be a tumor suppressor gene frequently mutated in GCs [5]. Our study of an independent Central European cohort aimed to confirm the specific phenotypic and genotypic characteristics of GC regarding expression of ARID1A. Our results showed partial or complete loss of expression in 14.7% of our cohort, which is almost identical with the prevalence of *ARID1A* mutations found

Table 2 Univariate and multivariate survival analysis

	Overall survival						Tumor-specific survival					
	Univariate Cox regression			Multivariate regression [a]		Cox	Univariate Cox regression			Multivariate regression [a]		Cox
	HR	95% CI	P	HR	95% CI	P	HR	95% CI	P	HR	95% CI	P
UICC stage (8th ed)			.000			.000			.000			.000
IIA/B vs I	1.876	1.212-2.903	.005	1.950	1.227-3.099	.005	2.528	1.451-4.404	.001	2.881	1.570-5.287	.001
IIIA/B/C vs I	4.221	2.831-6.293	.000	2.718	1.659-4.453	.000	6.109	3.662-10.193	.000	3.790	2.018-7.118	.000
IV vs I	7.542	4.870-11.681	.000	3.973	2.327-6.784	.000	10.794	6.251-18.639	.000	5.545	2.845-10.807	.000
Lymph node ratio	3.135	2.489-3.948	.000	1.797	1.291-2.503	.001	3.651	2.819-4.721	.000	1.958	1.337-2.867	.001
R status [R0 vs R1/2]	3.610	2.647-4.922	.000	2.506	1.790-3.508	.000	4.238	3.061-5.866	.000	2.749	1.931-3.913	.000
PD-L1 in immune cells	0.559	0.442-0.706	.000	0.602	0.471-0.770	.000	0.526	0.405-0.683	.000	0.609	0.463-0.801	.000

[a] Input variables: L, V, and R category; Laurén phenotype; UICC stage; lymph node ratio; tumor grade; MSI, PD-L1 (tumor and immune cells), and PD-1 status (immune cells); and Laurén phenotype group (diffuse/mixed versus intestinal/unclassified).

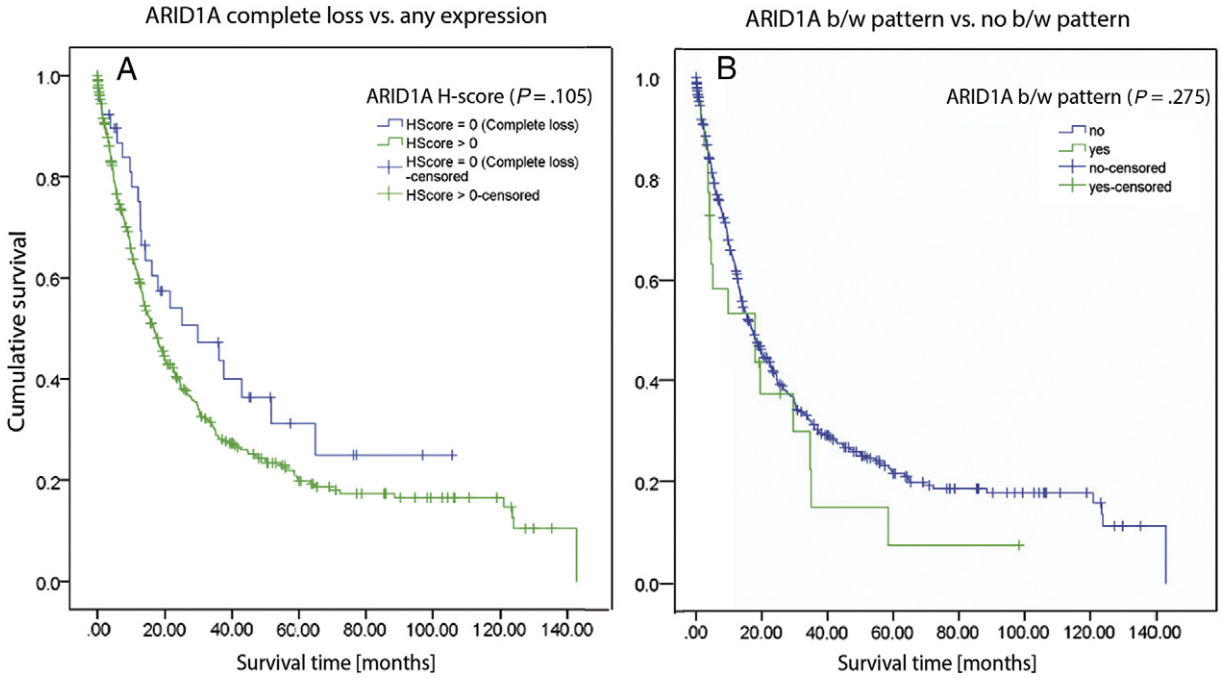

Fig. 3 Kaplan-Meier curves for ARID1A expression according to tumor-specific survival. A, GCs with a complete loss of ARID1A versus gastric carcinomas with any expression of ARID1A (not including b/w pattern). B, Gastric carcinomas with a partial, heterogeneous loss of ARID1A in a b/w expression pattern versus all others (not including complete loss).

recently by the Cancer Genome Atlas Research Network (TCGA) [5]. Interestingly, partial or complete loss of ARID1A expression correlated significantly with tumor type, nodal spread, lymph node ratio, and EBV and MSI status, further supporting the notion that loss of ARID1A is significant in terms of tumor biology and relates to molecular subtypes of GC. Recently synergistic inhibition of EZH2 in *ARID1A* mutated cancers has emerged as a potential form of targeted therapy in *ARID1A* mutated cancers [21].

4.1. ARID1A is expressed heterogeneously in GC

Regarding the putative diagnostic and clinical utility of novel biomarkers, previous studies have shown GC to be particularly prone to intratumoral heterogeneity [16,19,22-24]. This also applies to ARID1A. In this study, we found considerable diversity of ARID1A expression patterns: On the one hand, a vast majority of GCs (85.4%) showed a diffusely distributed expression pattern of different ARID1A staining intensities within the same tumor, which could be classified as a "gray scale" expression pattern. On the other hand, 43 (9.5%) GCs showed a complete loss of ARID1A expression and 23 cases harbored only a partial complete loss of ARID1A expression ranging from 1.0% to 88.0% of the entire tumor area (b/w pattern). This accounts to 35% of all tested GCs with partial or complete loss of ARID1A expression. In previous studies, we have made similar findings for HER2 [19], MET [25], *PIK3CA* [16], PD-L1 [24], and Ki67 [23] and classified this as intratumoral heterogeneity, which was demonstrated on both a genetic and protein level. Thus, the assessment of ARID1A loss in small tissue specimens, for example, biopsy or tissue micro arrays, is prone to sampling errors.

4.2. ARID1A loss is relevant for tumor biology irrespective of the percentage area

The heterogeneous expression of biomarkers may be associated with cancer biology in 2 ways, that is, existent or nonexistent. To further explore the impact of ARID1A loss, we correlated 4 groups (expression split at the median, complete loss, b/w heterogeneity, and complete loss and b/w combined) and noticed that any loss irrespective of the percentage area of the tumor is associated with clinicopathological patient characteristics. Two of our analyses support this contention: firstly, we were unable to find a correlation between the percentage area of ARID1A loss and clinicopathological patient characteristics in 23 digitalized GCs. Secondly, not only did both complete and partial loss (b/w) of ARID1A expression correlated with several clinicopathological patient characteristics in our main analysis; for most parameters, the correlations were even stronger when both groups were combined (Table 1). These findings suggest that, irrespective of the percentage area, any loss of ARID1A expression in GC is relevant.

The significance of ARID1A loss is further substantiated by loss of ARID1A in lymph node metastases: In lymph node metastases of patients with heterogeneous ARID1A expression in the primary tumor, we noted that 53.2%

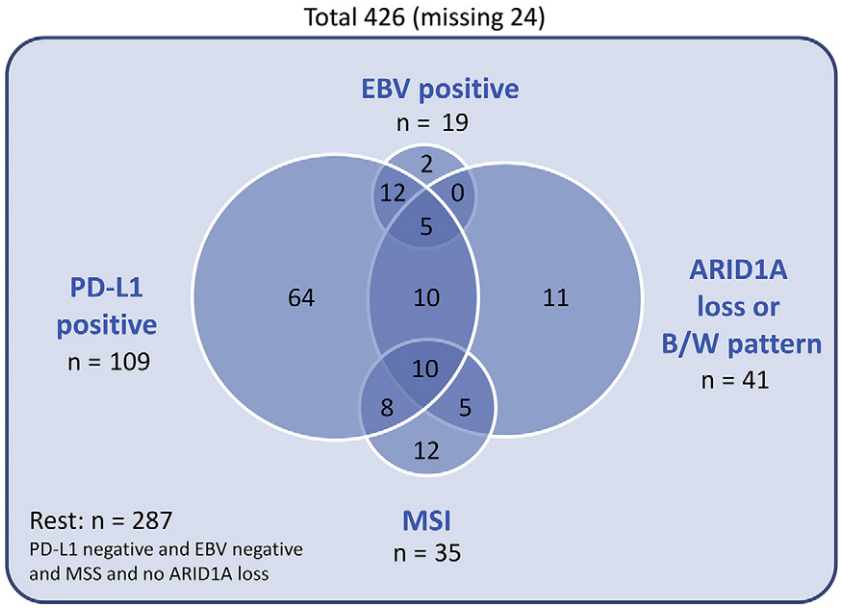

Fig. 4 The overlap of gastric carcinomas with complete loss of ARID1A or expression in a b/w pattern with gastric carcinomas with EBV positivity and MSI and PD-L1 expression is demonstrated in a Venn diagram.

showed a complete loss of ARID1A, 21.3% retained expression, and 25.5% showed a heterogeneous expression in the lymph node metastases (Supplementary Fig. 2). This observation leads to the conjecture that nodal metastases preferably stem from ARID1A negative GC subclones. This also correlates with the significantly higher lymph node ratio of ARID1A-negative GCs compared with ARID1A-positive GCs.

4.3. Genetic and epigenetic changes

It is generally accepted that ARID1A mutations in GC are truncating mutations that result in a loss of ARID1A protein expression. Nevertheless, we were unable to find an association between immunohistochemical ARID1A loss and genotype. Several factors may have influenced this outcome: ARID1A loss in GC not only might be due to mutations of the *ARID1A* gene but also might stem from epigenetic silencing, for example, by promoter hypermethylation [26]. The strong correlation of ARID1A loss with EBV we found suggests that such epigenetic changes need to be looked at as studies have found EBV infection to be associated with global CpG island hypermethylation [27]. Epigenetic effects would lead to discordance between mutational status and immunohistochemically detected protein levels, which has been reported in previous studies. For instance, Wang et al [11] found that although mutation of *ARID1A* led to immunohistochemically detectable loss of protein expression in most cases, there were also cases in which mutation status and H-score did not necessarily correlate. In our analysis, we were unable to detect hypermethylation of *ARID1A* CpG islands. However, the fact that only 7 GCs were suitable for mutational and hypermethylation testing limits the overall significance of the method. Protein loss also depends on mutation type [8], with a small percentage of mutations in noncoding loci showing loss of protein expression as well [9,10]. ARID1A protein loss might also be the result of posttranscriptional or posttranslational changes as Wiegand et al suggested for ovarian cancer [9,10].

4.4. ARID1A loss is associated with EBV and MSI GCs

GC's genetic complexity has recently been shown by comprehensive molecular profiling, and a molecular classification of GC was proposed, which categorizes 4 subtypes: EBV-associated GCs, MSI GCs, and chromosomal instable and genomically stable GCs [5]. In line with TCGA's findings and our second hypothesis, we found highly significant correlations of ARID1A loss (partial or complete) with EBV-associated GCs and MSI GCs (Fig. 4). ARID1A loss was also highly significantly associated with an intestinal and undifferentiated phenotype according to Laurén, subtypes which are associated with EBV and MSI as well as chromosomally instable molecular subtypes [5]. This observation suggests that ARID1A expression varies in the molecular subtypes of GC with a high association with EBV and MSI subtypes as well as chromosomally instable GCs, which show a lower mutation rate of ARID1A according to TCGA. This observation of ARID1A expression and mutational spectrum varying with GC subtype has been described in previous studies [11]. Although *HER2* and *MET* are frequently mutated genes in GCs with chromosomal instability according to TCGA [5], we could not detect a significant association of ARID1A loss with HER2 or MET status (Table 1).

4.5. Loss of ARID1A correlates with PD-L1 and PD-1 expression

In recent years, PD-L1, an immune checkpoint modulator, has become increasingly interesting as a therapeutic target in several different tumor entities and has been shown to correlate with patient prognosis in GC [24]. PD-1/PD-L1 checkpoint inhibitors are used to reenable immune response targeting cancerous cells. Thus, immune therapy for GC patients is subject of many current studies, for example, in the recent KEYNOTE-012 study, the anti-PD1 antibody pembrolizumab has been found to be a promising potential therapeutic agent for patients with recurrent or metastatic PD-L1–positive GC [28].

However, the issue of finding a viable predictive biomarker for immune therapy susceptibility prevails: Although PD-L1 has been established as a prognostic biomarker for immune therapy treatment in several other cancers (eg, NSCLC, malignant melanoma) [29], there is still debate about the suitability of PD-L1 immunostaining as predictive biomarker for GC [30]. Other biomarkers, such as MSI and EBV, have been found to be potential surrogates when screening for viable immune therapy candidates [31,32].

In a recently published study by Kim et al [33], PD-L1 expression was increased when ARID1A knockdown was initiated in GC cell lines. The authors suggested this to be mediated via activating AKT signaling. In line with the findings of this study and the results of a study by Ashizawa et al [13], our results confirm independently and in a Central European patient cohort the highly significant, inverse correlation of complete or partial (heterogeneous, b/w) loss of ARID1A expression with the expression of PD-L1 in tumor cells and PD-1 in tumor-infiltrating immune cells (Table 1; Fig. 4). Especially interesting is the notion of ARID1A and PD-L1 connection via activating AKT signaling, which might shed further light on the correlation of ARID1A, EBV, MSI, and PD-L1 in GC. The findings mentioned above suggest that ARID1A might be another potential surrogate marker for PD-L1 when identifying GC patients for potential immune therapy, which should be confirmed in future studies.

4.6. Heterogeneous ARID1A expression is associated with *PIK3CA* mutation

Although there is significant association of partial (heterogeneous) ARID1A loss and *PIK3CA* mutation, the connection may be mediated by EBV, which has also been described by authors of previous studies [34]. The link between ARID1A loss and *PIK3CA* because interesting as *PIK3CA* is a possible therapeutic target in EBV-associated cancers: among others, PX-866, an oral irreversible phosphatidylinositol 3-kinase inhibitor, has been found to be a promising candidate for treatment of advanced EBV-associated cancers in a phase I clinical trial [35]. Interestingly, only heterogeneous loss of ARID1A correlated strongly with *PIK3CA* mutation status in our study; thus, when ARID1A heterogeneous expression is noted in GC, further investigation of *PIK3CA* genotype should possibly be considered in light of *PIK3CA*'s possible future use as therapeutic target in advanced EBV-associated tumors.

5. Conclusions

In conclusion, we were able to prove our tested hypotheses in this study: intratumoral heterogeneity, a well-known feature of GC, also applies to ARID1A expression with a specific b/w staining pattern in 23 cases (5.1%). Our results suggest that, irrespective of the percentage area, any complete cellular loss of ARID1A expression is relevant in terms of tumor biology: Partial or complete loss of ARID1A expression occurs in 14.7% of GCs and is associated with molecular subtype (EBV, MSI), PD-L1 status, *PIK3CA* genotype as well as nodal metastases, which preferably stem from ARID1A-negative GC subclones. Furthermore, ARID1A varies between the molecular subtypes of GC, with significant association with intestinal and undifferentiated phenotypes according to Laurén. We found no association with HER2 or MET. Although our analysis did not show significant correlation of ARID1A expression with patient survival, the observed heterogeneous expression may impact its diagnostic utility as a predictive biomarker, which should be considered in future studies. Another point worth considering in future studies is the highly significant correlation of ARID1A loss with PD-L1 expression which has recently been shown in other studies for different patient cohorts and might hold potential for a combined anti–PD-L1/ARID1A therapy.

Acknowledgment

We wish to thank Deniza Hajzeri for her excellent technical assistance.

Compliance with ethical standards

This study was performed according to the Declaration of Helsinki. Ethical approval was obtained from the local ethical review board (D 453/10). After study inclusion, data from all patients were pseudonymized.

Contributions

Study concept and design were done by J. M. T. and C. R. Surgical pathological data were acquired by J. M. T., C. H., and C. R. The data were analyzed and interpreted by J. M. T., H. M. B., and C. R. Drafting of the manuscript and critical

revision of the manuscript for important intellectual content were done by all authors. Administrative, technical, or material support was provided by S. K. and C. R. The study was supervised by C. R.

References

[1] Laurén P. The two histological main types of gastric carcinoma: diffuse and so-called intestinal-type carcinoma. an attempt at a histo-clinical classification. Acta Pathol Microbiol Scand 1965;64:31-49.

[2] Bosman FT, Carneiro F, Hruban RH, Theise ND. WHO classification of tumors of the digestive system. . 4th ed.Lyon: IARC; 2010.

[3] Wang K, Yuen ST, Xu J, et al. Whole-genome sequencing and comprehensive molecular profiling identify new driver mutations in gastric cancer. Nat Genet 2014;46:573-82. https://doi.org/10.1038/ng.2983.

[4] Kim KJ, Jung HY, Oh MH, et al. Loss of ARID1A expression in gastric cancer: correlation with mismatch repair deficiency and clinicopathologic features. J Gastric Cancer 2015;15:201-8. https://doi.org/10.5230/jgc.2015.15.3.201.

[5] The Cancer Genome Atlas Network (TCGA). Comprehensive molecular characterization of gastric adenocarcinoma. Nature 2014;513:202-9. https://doi.org/10.1038/nature13480.

[6] Chandler RL, Brennan J, Schisler JC, et al. ARID1a-DNA interactions are required for promoter occupancy by SWI/SNF. Mol Cell Biol 2013;33:265-80. https://doi.org/10.1128/MCB.01008-12.

[7] Hodges C, Kirkland JG, Crabtree GR. The many roles of BAF (mSWI/SNF) and PBAF complexes in cancer. Cold Spring Harb Perspect Medicine 2016;6. https://doi.org/10.1101/cshperspect.a026930.

[8] Guan B, Gao M, Wu CH, Wang TL, Shih IeM. Functional analysis of in-frame indel ARID1A mutations reveals new regulatory mechanisms of its tumor suppressor functions. Neoplasia 2012;14:986-93. https://doi.org/10.1593/neo.121218.

[9] Wu JN, Roberts CW. ARID1A mutations in cancer: another epigenetic tumor suppressor? Cancer Discov 2013;3:35-43. https://doi.org/10.1158/2159-8290.CD-12-0361.

[10] Wiegand KC, Shah SP, Al-Agha OM, et al. ARID1A mutations in endometriosis-associated ovarian carcinomas. N Engl J Med 2010;363:1532-43. https://doi.org/10.1056/NEJMoa1008433.

[11] Wang K, Kan J, Yuen ST, et al. Exome sequencing identifies frequent mutation of ARID1A in molecular subtypes of gastric cancer. Nat Genet 2011;43:1219-23. https://doi.org/10.1038/ng.982.

[12] Ibarrola-Villava M, Llorca-Cardeñosa MJ, Tarazona N, et al. Deregulation of ARID1A, CDH1, cMET and PIK3CA and target-related microRNA expression in gastric cancer. Oncotarget 2015;6:26935-45. https://doi.org/10.18632/oncotarget.4775.

[13] Ashizawa M, Saito M, Min AKT, et al. Prognostic role of ARID1A negative expression in gastric cancer. Sci Rep 2019;9:6769. doi:https://doi.org/10.1038/s41598-019-43293-5.

[14] Trizzino M, Barbieri E, Petracovici A, et al. The tumor suppressor ARID1A controls global transcription via pausing of RNA polymerase II. Cell Rep 2018;23:3933-45. https://doi.org/10.1016/j.celrep.2018.05.097.

[15] Guan B, Wang TL, Shih IM. ARID1A, a factor that promotes formation of SWI/SNF-mediated chromatin remodeling, is a tumor suppressor in gynecologic cancers. Cancer Res 2011;71:6718-27. https://doi.org/10.1158/0008-5472.CAN-11-1562.

[16] Böger C, Krüger S, Behrens HM, et al. Epstein-Barr virus–associated gastric cancer reveals intratumoral heterogeneity of PIK3CA mutations. Ann Oncol 2017;28:1005-14. https://doi.org/10.1093/annonc/mdx047.

[17] Warneke VS, Behrens HM, Haag J, et al. Prognostic and putative predictive biomarkers of gastric cancer for personalized medicine. Diagn Mol Pathol 2013;22:127-37. https://doi.org/10.1097/PDM.0b013e318284188e.

[18] Mathiak M, Warneke VS, Behrens HM, et al. Clinicopathologic characteristics of microsatellite instable gastric carcinomas revisited: urgent need for standardization. Appl Immunohistochem Mol Morphol 2017;25:12-24. https://doi.org/10.1097/PAI.0000000000000264.

[19] Warneke VS, Behrens HM, Böger C, et al. Her2/neu testing in gastric cancer: evaluating the risk of sampling errors. Annal. Oncologia 2013;24:725-33. https://doi.org/10.1093/annonc/mds528.

[20] Metzger ML, Behrens HM, Böger C, et al. MET in gastric cancer—discarding a 10% cutoff rule. Histopathology 2016;68:241-53. https://doi.org/10.1111/his.12745.

[21] Bitler BG, Aird KM, Garipov A, et al. Synthetic lethality by targeting EZH2 methyltransferase activity in ARID1A-mutated cancers. Nat Med 2015;21:231-8. https://doi.org/10.1038/nm.3799.

[22] Chen K, Yang D, Li X, et al. Mutational landscape of gastric adenocarcinoma in Chinese: implications for prognosis and therapy. Proc Natl Acad Sci U S A 2015;112:1107-12. https://doi.org/10.1073/pnas.1422640112.

[23] Böger C, Behrens HM, Röcken C. Ki67—an unsuitable marker of gastric cancer prognosis unmasks intratumoral heterogeneity. J Surg Oncol 2016;113:46-54. https://doi.org/10.1002/jso.24104.

[24] Böger C, Behrens HM, Mathiak M, et al. PD-L1 is an independent prognostic predictor in gastric cancer of Western patients. Oncotarget 2016;7:24269-83. https://doi.org/10.18632/oncotarget.8169.

[25] Choi J, Lee HE, Lee HS, et al. Evaluation of intratumoral and intertumoral heterogeneity of MET protein expression in gastric cancer. Appl Immunohistochem Mol Morphol 2018;26:445-53. https://doi.org/10.1097/PAI.0000000000000448.

[26] Zhang X, Sun Q, Shan M, et al. Promoter hypermethylation of ARID1A gene is responsible for its low mRNA expression in many invasive breast cancers. PLoS One 2013;8:e53931. https://doi.org/10.1371/journal.pone.0053931.

[27] Morales-Sanchez A, Fuentes-Panana EM. Epstein-Barr virus–associated gastric cancer and potential mechanisms of oncogenesis. Curr Cancer Drug Targets 2017;17:534-54. https://doi.org/10.2174/1568009616666160926124923.

[28] Muro K, Chung HC, Shankaran V, et al. Pembrolizumab for patients with PD-L1–positive advanced gastric cancer (KEYNOTE-012): a multicentre, open-label. phase 1b trial Lancet Oncol 2016;17:717-26. https://doi.org/10.1016/S1470-2045(16)00175-3.

[29] Salmaninejad A, Valilou SF, Shabgah AG, et al. PD-1/PD-L1 pathway: Basic biology and role in cancer immunotherapy. J Cell Physiol 2019;234:16824–37. doi:https://doi.org/10.1002/jcp.28358.

[30] Koemans WJ, Chalabi M, van Sandick JW, van Dieren JM, Kodach LL. Beyond the PD-L1 horizon: in search for a good biomarker to predict success of immunotherapy in gastric and esophageal adenocarcinoma. Cancer Lett 2019;442:279–86. doi:https://doi.org/10.1016/j.canlet.2018.11.001.

[31] Le DT, Durham JN, Smith KN, et al. Mismatch repair deficiency predicts response of solid tumors to PD-1 blockade. Science 2017;357:409-13. https://doi.org/10.1126/science.aan6733.

[32] Kim ST, Cristescu R, Bass AJ, et al. Comprehensive molecular characterization of clinical responses to PD-1 inhibition in metastatic gastric cancer. Nat Med 2018;24:1449-58. https://doi.org/10.1038/s41591-018-0101-z.

[33] Kim YB, Ahn JM, Bae WJ, Sung CO, Lee D. Functional loss of ARID1A is tightly associated with high PD-L1 expression in gastric cancer. Int J Cancer 2019;15:916-26. https://doi.org/10.1002/ijc.32140.

[34] Zhou H, Tan S, Li H, Lin X. Expression and significance of EBV, ARID1A and PIK3CA in gastric carcinoma. Mol Med Rep 2019;19:2125-36. https://doi.org/10.3892/mmr.2019.9886.

[35] Hong DS, Bowles DW, Falchook GS, et al. A multicenter phase I trial of PX-866, an oral irreversible phosphatidylinositol 3-kinase inhibitor, in patients with advanced solid tumors. Clin Cancer Res 2012;18:4173-82. https://doi.org/10.1158/1078-0432.CCR-12-0714.